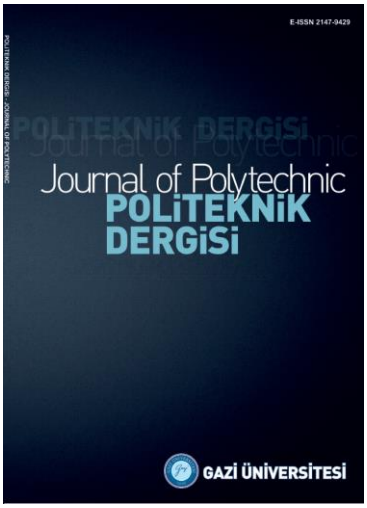

POLİTEKNİK DERGİSİ

JOURNAL of POLYTECHNIC

ISSN: 1302-0900 (PRINT), ISSN: 2147-9429 (ONLINE)
URL: http://dergipark.org.tr/politeknik

Investigation of discharge characteristics of hinges produced with 3D printing for prosthetic fingers

Protez parmaklar için 3B baskı ile üretilmiş menteşelerin deşarj karakteristiğinin incelenmesi

***Yazar(lar) (Author(s))**: Mine SEÇKİN[1], Ahmet Çağdaş SEÇKİN[2], Necla YAMAN TURAN[3]*

ORCID[1]: 0000-0002-9564-1534

ORCID[2]: 0000-0002-9849-3338

ORCID[3]: 0000-0001-7432-4137

Bu makaleye şu şekilde atıfta bulunabilirsiniz(To cite to this article): Seçkin M., Seçkin A. Ç. ve Yaman Turan N., "Investigation of discharge characteristics of hinges produced with 3D printing for prosthetic fingers", ***Politeknik Dergisi***, 24(2): 575-583, (2021).

Erişim linki (To link to this article): http://dergipark.org.tr/politeknik/archive

DOI: **10.2339/politeknik.698316**

Investigation of Discharge Characteristics of Hinges Produced with 3D Printing for Prosthetic Fingers

Highlights

- *Investigation of 3D printing hinges discharge characteristics*
- *Investigation of 3D printing hinges energy consumption characteristics*
- *Comparsion for 3D printing parameter effects*
- *Decision of optimized 3d printed hinge parameters for prosthetic fingers*

Graphical Abstract

Hinges with different printing parameters are produced and their discharge characteristics and energy consumption are investigated.

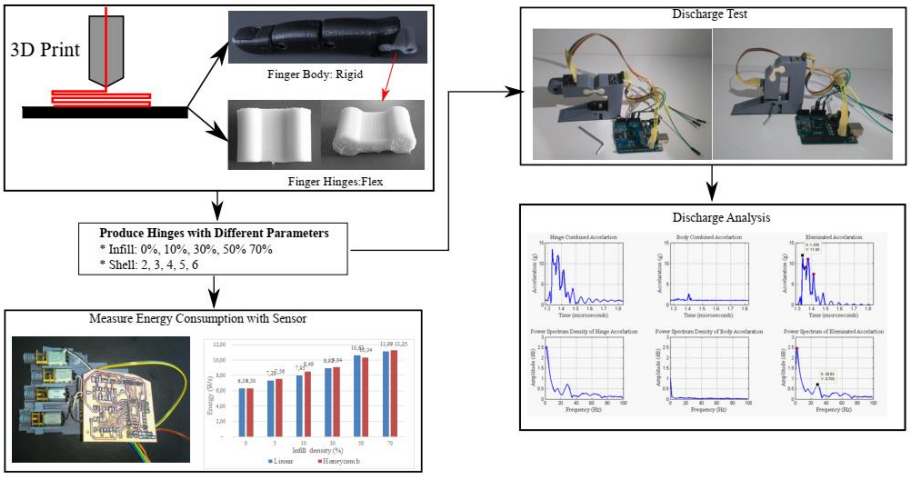

Figure. Graphical representation of the methods and tests used in the study

Aim

This study aims to determine the discharge characteristics of the flexible hinges used in prosthetic hands and fingers according to the production techniques and to determine the most appropriate hinge production parameters. The speed of the opening process and the energy consumption during the closing process directly depend on the structure of the flexible hinge.

Design & Methodology

In the method of the study, primarily flexible hinge samples are produced using different printing parameters. In the next step, a finger-like test system is designed that uses accelerometers to measure discharge oscillations on the fingers. The test mechanism has a body and a free accelerometer. The body sensor is used to distinguish body vibrations transmitted to the free accelerometer.

Originality

There is a lack of study about characteristics and behaviors researches of 3d printed hinges. This study fills the gap in the decision of optimized 3d printed hinge parameters for prosthetic fingers.

Findings

It has been concluded that the hinge, which has the highest energy storage capacity at the lowest cost, will have a honeycomb filling shape, 30% filler, and four shells.

Conclusion

This study will be a light for wearable machines that include hinge while estimating the mechanical behaviors and optimizing its mechanical parts. If a fast aggregation (which is an important feature for prostheses) is desired, a hinge that provides a high frequency can be preferred.

Declaration of Ethical Standards

The authors of this article declare that the materials and methods used in this study do not require ethical committee permission and/or legal-special permission.

Protez Parmaklar için 3B Baskı ile Üretilmiş Menteşelerin Deşarj Karakteristiğinin İncelenmesi

Araştırma Makalesi / Research Article

Mine SEÇKİN[1*], Ahmet Çağdaş SEÇKİN[2], Necla YAMAN TURAN[1]

[1]Mühendislik Fakültesi, Tekstil Mühendisliği Bölümü, Uşak Üniversitesi, Türkiye
[2]Teknik Bilimler Meslek Yüksek Okulu, Mekatronik Bölümü, Uşak Üniversitesi, Türkiye

(Geliş/Received : 03.03.2020; Kabul/Accepted : 06.05.2020)

ÖZ

Esnek menteşeler, yumuşak veya esnek malzemelerden yapılmış eklem mekanizmalarıdır. Bu çalışmanın amacı, protez el ve parmaklarda kullanılan esnek menteşelerin deşarj özelliklerinin üretim tekniklerine göre değişim karakteristiklerini çıkarma ve en uygun menteşe üretim parametrelerini belirlemektir. Esnek menteşeler kullanan parmak tasarımlarında, açma işleminin hızı ve kapatma işlemi sırasında enerji tüketimi doğrudan esnek menteşenin yapısına bağlıdır. Bu nedenle, esnek menteşe yapısının değişimi ile deşarjı arasındaki ilişkiyi salınım ve enerji ihtiyacı açısından incelemek önemlidir. Çalışmanın yönteminde farklı baskı parametreleri kullanılarak esnek menteşe örnekleri üretilmiştir.Sonrasında parmaklardaki deşarj salınımlarını ölçmek için ivme ölçerler kullanan parmak benzeri bir test sistemi tasarlanmıştır. Test mekanizması bir gövdeye ve serbest bir ivmeölçere sahiptir. Gövde sensörü, serbest ivme ölçere iletilen gövde titreşimlerini ayırt etmek için kullanılır. Test sistemi ile yapılan ölçümler sonucunda, petek şeklinin, şekli doldurmak açısından doğrusal şekle göre daha yüksek frekanslı titreşimler ürettiği görülmektedir. Bu, petek dolgusunun esneme sonucu daha yüksek miktarda enerji depolayabildiğini gösterir. İç dolgu yüzdesi veya dış kabukların sayısı arttıkça, serbest bırakıldığında esnek menteşenin titreşim sıklığı daha yüksek bulunmuştur. En düşük maliyetle en yüksek enerji depolama kapasitesine sahip menteşenin petek dolgu şekli, % 30 dolgu ve dört kabukla sahip olacağı sonucuna varılmıştır. Son olarak, parmak kapatma işlemleri için tüketilen gücü ölçen bir sistem sunulmuştur. Menteşeli enerji tüketim seviyeleri sonucunda dolgu yoğunluğu ve kabuk değeri sayısı arttıkça enerji tüketiminin arttığı gözlenmiştir. Bu değerlerin salınım değerleri ile uyumlu olduğu görülmektedir. Bu sistemle, gelecekte 3b baskı ile üretilmesi planlanan robotik protez parmak uygulamasında parametre seçiminde kullanılması hedeflenmektedir.

Anahtar Kelimeler: Esnek menteşeler, menteşe test cihazı, 3B baskı, eklemeli üretim, protez parmak.

Investigation of Discharge Characteristics of Hinges Produced with 3D Printing for Prosthetic Fingers

ABSTRACT

Flexible hinges are joint mechanisms made of soft or flexible materials. The aim of this study is to determine the discharge characteristics of the flexible hinges used in prosthetic hands and fingers according to the production techniques and to determine the most appropriate hinge production parameters. The speed of the opening process and the energy consumption during the closing process directly depend on the structure of the flexible hinge. For this reason, it is important to examine the relationship between the change of the flexible hinge structure and its discharge in terms of oscillation and energy requirement. In the method of the study, primarily flexible hinge samples are produced using different printing parameters. In the next step, a finger-like test system is designed that uses accelerometers to measure discharge oscillations on the fingers. The test mechanism has a body and a free accelerometer. The body sensor is used to distinguish body vibrations transmitted to the free accelerometer. As a result of the measurements made with the test system, it is observed that the honeycomb shape produced higher frequency vibrations than the linear shape in terms of filling the shape. This indicates that the honeycomb filler can store a higher amount of energy as a result of stretching. As the percentage of inner fill or the number of outer shells increased, the frequency of vibration of the flexible hinge when released is found to be higher. It has been concluded that the hinge, which has the highest energy storage capacity at the lowest cost, will have a honeycomb filling shape, 30% filler, and four shells. Finally, a system that measures the power consumed for finger closing operations is presented. As a result of energy consumption levels with hinges, it has been observed that energy consumption increases as infill density and number of shell values increase. It is seen that these values are compatible with oscillation values. With this system, it is aimed to be used for parameter selection in robotic prosthetic finger application which is planned to be produced by 3D printing in the future.

Keywords: Flexible hinge, hinge tester, 3d printing, additive manufacturing, prosthetic finger.

1. INTRODUCTION

The flexible hinge is a type of joint mechanism that is made of flexible materials. The advantages of the flex hinges are no friction losses, no need to lubricate, no hysteresis, and compactness, capacity to be utilized in small scale applications, ease of fabrication, and low or no maintenance. On the other hand, there are drawbacks such as the level of rotation is low, an axis of the rotation is not pure due to production techniques and flex materials, rotation center is not fixed during the rotation

**Sorumlu Yazar (Corresponding Author)*
e-posta : mine1seckin@gmail.com

because of the combined load/ force, sensitivity to temperature because of the flexible materials[1]. The bending strength and the number of axes vary according to the shape and region thickness of the flexible hinges in the bending region. There are three main hinge types which are shown in Figure 1, respectively, single axis, multiple-axis (revolute), and two-axis[1], [2]. (Figure 1.). A single-axis flexible hinge works in 2D and other types of work in 3D [3]. Also, Mutlu et. al categorized the flexible hinges as symmetric and non-symmetric in terms of their geometry. The symmetric flexible hinge has a geometrical symmetry based on their longitudinal axis (Figure 2.) and a non-symmetric flexible hinge has one flat side and one with a designated geometrical shape [3].

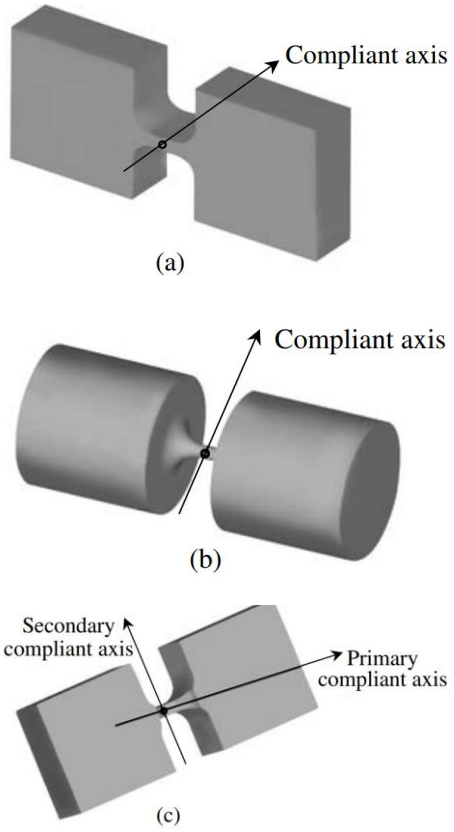

Figure 1. Flexible Hinge Configurations (a) Single-Axis, (b) Multiple Axis (c) Two Axis [1].

Hinge production types include end-milling, electro-discharge machining, laser cutting, metal stamping, or photolithographic techniques for microelectromechanical systems, and turning or precision casting[1], [4]–[7]. Suzuki et.al. produced hinges by using conventional silicon micromachining techniques[8]. Cai et.al produced a flexible hinge wire electrical discharge machining method [9]. 3d printer is relatively a new production technology compared to the other manufacturing techniques. The advantages of the 3d printing method are minimum material waste, easy to produce prototypes, no need for a mold, easy to reproduce, changeable fillet, and also possible to recycle. Usage areas of flexible hinges are automotive, aviation, and robotics industries, and biomedical industry [1], [10]. While producing a flex hinge, a sensor can be embedded into hinges, so a flex hinge can be used as a sensor [11]–[13].

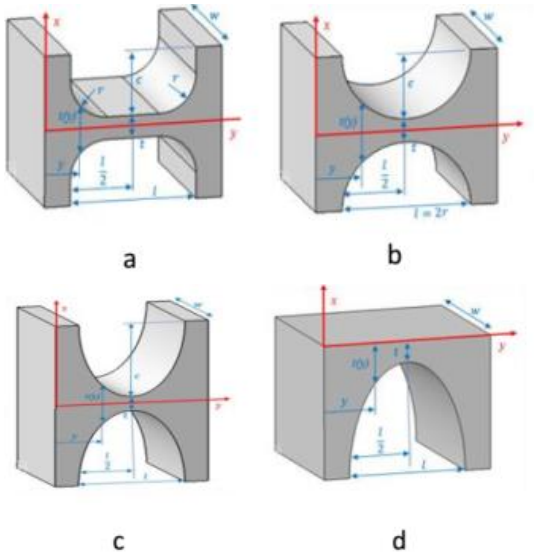

Figure 2. Geometric Parameters of Single Axis Flexible Hinges (a) Symmetric Corner Filleted, (b) Circular, (c) Elliptical, (d) Non-Symmetric Elliptical [3].

Li et.al and Qin et.al. produced a hinge for Piezoelectric actuators' which have been widely used in micro-/nano positioning, super-precision machining, precision optics engineering, electronic microscope, biomedical engineering [14], [15].

In scientific studies, Lotti et. al. emphasize the importance of hinge design and materials. For example, two types of articulated fingers are designed and compared in previous works. Their fingers are integrated flexible which are made of the same material as hinges and phalanges. They gave the kineostatic models of the hinge. They used Politetrafloretilen (PTFE) because of its good mechanical properties manufacturability, low friction, and wear resistance. Lotti et.al. tested prototypes to the characterization of the structural behavior and the evaluation of the achievable performance [16]. Miloradovic et.al. used elastic joints instead of conventional hinge joints in their robotic finger and mentioned the grasping ability of hinge types. They explained that the finger became more energy efficient with elastic hinges. They used the optoelectronic angular sensor for angular measurement[17]. Ogahara et.al. used elastic torsion springs and hinges in their mechanisms [18]. Biagiotti et. al. used a compliant elastic hinge that can allow relative motion of chains. They mentioned that one of the major problems is the optimization of hinges. Optimization related to the topological definition, material choice, correct sizing to obtain an acceptable lifetime. According to them, low bending stiffness is desirable but at the same time, torque and compression loads should not determine the excessive strain. They

showed an analytical study and they gave ideal model of the hinges [19].

Zhu et.al introduced various types of flexible hinges and implemented them in a variety of fields in accord with their superior performances. They showed a schematic of typical flexible hinges such as circular-axis hinge, single-directional hinge, and bi-directional hinge [20]. In [20]the authors described the development of a humanoid robot hand based on an endoskeleton made of rigid links connected with elastic hinges, and they used spring as an elastic hinge. Carrozza et. al. mentioned the living hinges in robotic hands. They explained living hinge as thin sections of polymer that connect two segments of a part to keep them together and allow the part to be opened and closed. They exemplify polypropylene and polyethylene materials for hinges [21].

The study aims to examine the discharge characteristics of flexible hinges used in prosthetic fingers. In finger designs using flexible hinges, finger closing movement is performed by motors, while the finger opening movement is performed by a flexible hinge. The speed of the opening process and the power consumption during the closing process directly depend on the structure of the flexible hinge. For this reason, it is important to examine the relationship between the change of the flexible hinge structure and its discharge in terms of oscillation and energy requirement.

In this paper, a single-axis flexible hinge for wearable machines, especially finger prostheses, is produced by fused deposition manufacturing (FDM) method. Although this method has a lot of advantages, it has not been a serial producing method yet. There is not any study about characteristics and behaviors researches of 3d printed hinges in literature. This study aims to close the gap in the literature and to be a reference in choosing the hinge to be used in future wearable robots. Especially we need these characteristics for the 3d printed wearable hand prostheses' fingers. It is important to estimate the mechanical behavior and optimize its mechanical parts. In this study, forces and vibrations generated by hinges that have different print characteristics are measured with the accelerometer and obtained results are presented.

This paper presents the effect of infill parameters and the number of shells on 3d printed flexible hinges for the design of a robotic hand based on this concept. Material and method are explained in section two. Experimental results are given in section three. And final remarks and plans for future activity are reported in section four.

2. MATERIAL AND METHOD

The study aims to examine the discharge characteristics of flexible hinges used in prosthetic fingers. In finger designs using flexible hinges, finger closing movement is performed by motors, while the finger opening movement is performed by a flexible hinge. The speed of the opening process and the energy consumption during the closing process directly depend on the structure of the flexible hinge. For this reason, it is important to examine the relationship between the change of the flexible hinge structure and its discharge in terms of oscillation and energy requirement. The prosthetic hand and finger to use hinges are shown in Figure 3. In the method of the study, primarily flexible hinge samples are produced using different printing parameters. In the next step, a finger-like test system is designed that uses accelerometers to measure discharge oscillations on the fingers. Finally, a system that measures the power consumed for finger closing operations is presented.

Figure 3. Prosthetic Hand and Finger with Flexible Hinge

2.1. The Flexible Hinge Design and Production

3D design of hinge and experimental setup which are shown in Figure 4 is made with the "FreeCAD" program. These designs are manufactured in the "MakerBot Replicator 2" 3D printer. Hinge's dimensions are designed to be the same as shown in Figure 4. Each flexible hinge is manufactured in a 3 cm width. 3D printed hinges are produced from the flexible filament (Ninja flex PLA) which are shown in Figure 5. While processing parameters of the printer are kept constant and infill density, infill pattern, and the number of shell specifications are changed to examine the effect on the hinges properties. Printer's constant settings are listed as follows:

- The technical specifications of the flexible filament of the Ninja flex brand are written to melt between 190ºC and 220ºC. However, it is observed that inter-layer retention is difficult at low temperatures during production and the desired hinge shapes could not be obtained. Therefore, the extruder temperature is set to 220 ºC.
- Platform temperature is at room temperature. Travel speed is the speed at which the printing head moves while extruding the filament to create the physical representation of the 3D model and its value is 150mm/s and Z-axis

- Travel speed is 23 mm/s.
- Minimum layer duration is the minimum time required for a layer to freeze, and the production of a top layer is not started before this period is completed. This value is 5.0s in this study.
- Filament cooling fan speed is 0.5 mm/s, print speed is 40mm/s.
- Infill layer height is the main parameter that affects the print quality as it sets the thickness of each layer that is being printed and its value is 0.20 mm, roof thickness is 0.60 mm, floor thickness is 0.60 mm.

The parameters to be analyzed in experimental samples are infill density, infill pattern, and the number of shells. Infill density defines the amount of material inside the print. To save time and material in production with 3d printers, the objects to be produced are not printed as full fill, but instead, an infill pattern is created on the inside to ensure body integrity. Infill pattern can be honeycomb (hexagonal) or linear which is shown in Figure 6. Numbers of shells is a value that sets the number of outlines printed on each layer of the object. The more shells there are, the stronger the printed object is, so setting a higher number of essentially shells make the printed part with denser outside walls. As the number of shells increases, the number of outer walls of the printed object increases. This ensures that the part is more robust.

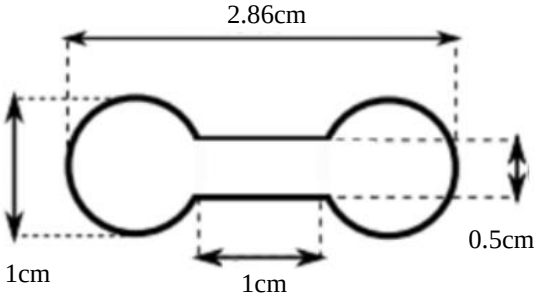

Figure 4. Hinge Dimensions

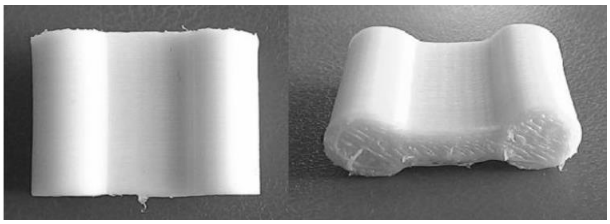

Figure 5. A 3D Printed Flexible Hinge

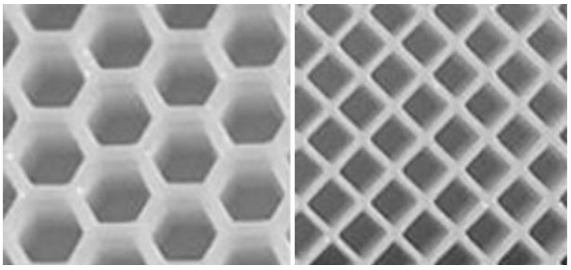

(a) (b)

Figure 6. Infill Patterns (a) Honeycomb, (b) Linear

2.2. Flexible Hinge Test System Design

The flexible hinge test system is shown in Figure 7 and consists of a microcontroller, gyroscopes, and accelerometer. To ensure the similarity of the finger, the index finger dimensions of the prosthetic hand are taken as reference. An accelerometer is an electromechanical device that measures acceleration. These forces may be static or dynamic - caused by moving or vibrating the accelerometer [22]. Inertial measurement unit (IMU) sensors-MPU6050 is chosen as an accelerometer, because of its easy implementation and low cost. There are two IMU sensors in the test system and both are connected to the microcontroller via I2C protocol. Reference IMU addressed as 0x68 (connect AD0 pin to ground) and dynamic IMU sensor addressed as 0x69 (connect AD0 pin to 5V). Each IMU sensor is configured to sense to 16g acceleration. Data is sent to the computer via UART (Universal Asynchronous Receiver Transmitter) with 115200 baud rates. The sampling time of the IMU sensors is 0.1s. Incoming data is collected with a Python program. After collecting data from IMU sensors, an analysis program that is written with Python with numpy, scipy, and matplotlib libraries extracts analysis features.

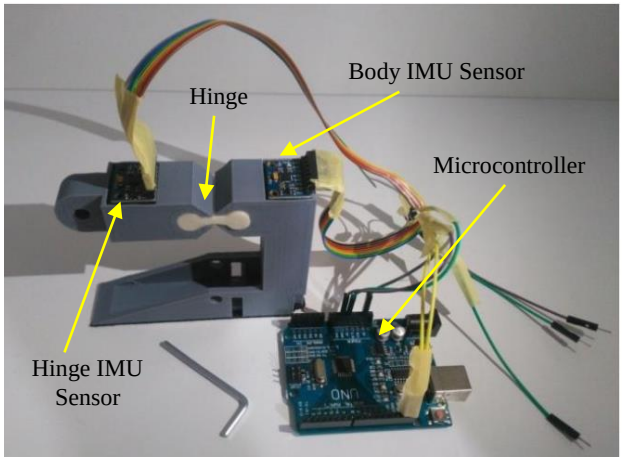

(a)

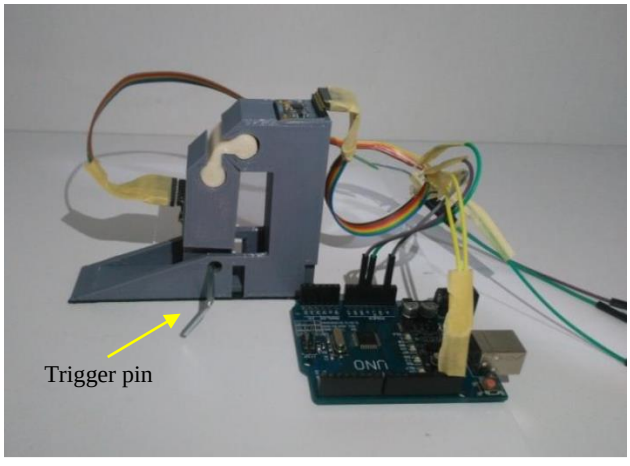

(b)

Figure 7. Flexible Hinge Test System (a) in free and (b) in tension

The flow chart of the program is given in Figure 8. The features are combined from one-time domain and two frequency domain values. We use two IMU sensors to eliminate body vibrations. The elimination process is to calculate combined acceleration values of both sensors and after this to subtract body IMU values from hinge IMU values. After the elimination of body vibrations, the time domain feature value is calculated as the first peak value of eliminated acceleration. Frequency domain features are extracted by using spectral power density and they include two stages. The first stage is a 20Hz high pass filter because of denying the noise signal of the IMU sensor. The second stage is first to peak magnitude and frequency value over 20Hz.

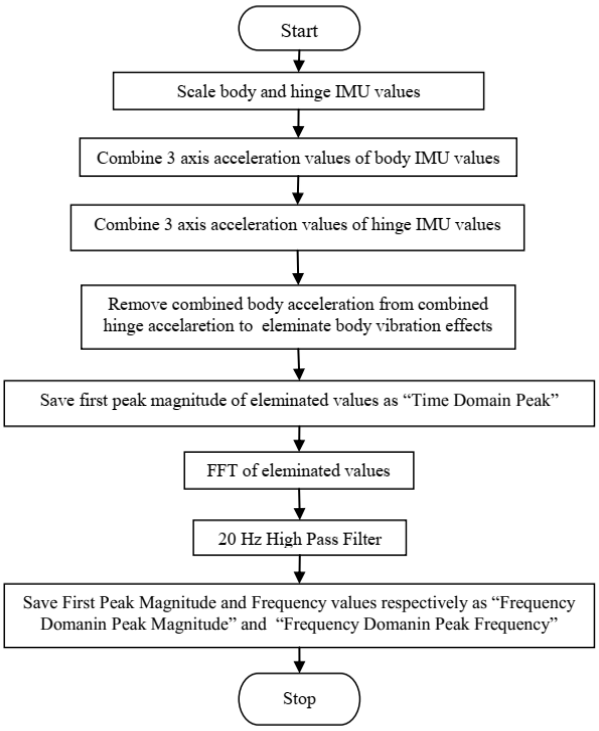

Figure 8. Flexible Hinge Test System Flowchart

2.3. Energy Consumption Measurement System for Finger Closing

The system designed for energy measurement is shown in Figure 9 for one finger. The actual version of the system is presented in Figure 10. Power supply, microcontroller, current sensor, H-bridge motor driver, DC motor, pulley, and limit switch are used in the measurement system. The power supply used in the operation of the system is a 3.3V 2500mAh LiPo battery. All units in the system are powered by this power supply. Arduino Pro-Mini is used as a microcontroller. The microcontroller H-bridge type L298N motor drives the drive with full power until the limit switch is triggered. The direct current sensor takes continuous measurement during the driving process and the energy consumed is measured in this way.

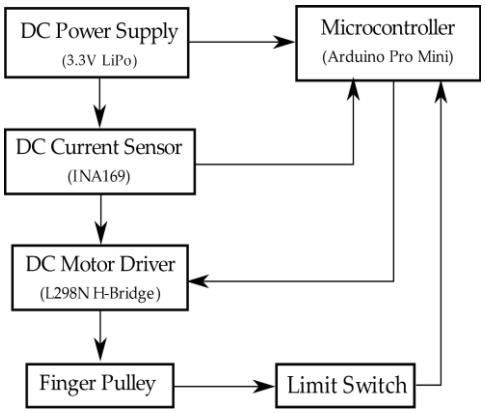

Figure 9. Energy Measurement System

Figure 10. Prosthetic hand with Flexible Hinges

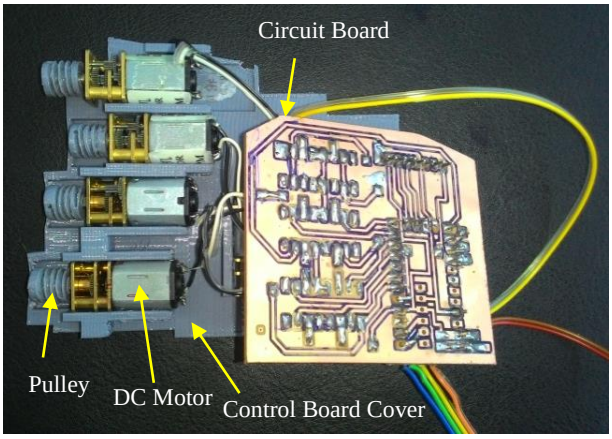

Figure 11. Electronic Circuit for Prosthetic Hand fingers

3. RESULTS AND DISCUSSION

In this study, 16 types of hinges were produced and a total of 80 pieces, 5 of each type. The properties of the samples are shown in Table 1. As shown in Table 1, the inner filler densities are chosen as 0, 5, 10, 30, 50 and 70% infill density samples have not been tested because they have lost their elasticity. The inner fill pattern is honeycomb and linear. However, the internal pattern is not applied to the samples specified here as none. Only two shells are used for the samples with internal patterns. Then, to see the effects of the number of shells, the number of shells is tested as 2, 3, 4,5, and 6 in hollow samples. The table also presents the average weights of the samples in grams.

As an example of the measurements made on samples, Figure 12 is presented. As an example of test result graphics of experiment 01 are shown in Figure 12. The combined accelerations in the time domain of hinge and the body IMU sensors are given in Figure 12 (a) and (b), respectively. Eliminated acceleration is obtained by subtracting the body IMU signal from the hinge IMU signal and the result is presented in Figure 12 (c). The power spectral density (PSD) is obtained by the frequency domain Fourier transforms. The PSD of the hinge and the body IMU sensors are given in Figure 12 (c) and (d) respectively. Eliminated PSD is obtained by subtracting the body IMU signal from the hinge IMU signal and the result is presented in Figure 12 (c).

Table 1. Experimental Production List

Ex. No	Infill Pattern	Infill Density %	Nof Shell	Weight (gr)
e1	Honeycomb	0%	2	3.00
e2	Honeycomb	5%	2	3.16
e3	Honeycomb	10%	2	3.22
e4	Honeycomb	30%	2	3.38
e5	Honeycomb	50%	2	3.70
e6	Honeycomb	70%	2	4.27
e7	Linear	0%	2	3.03
e8	Linear	5%	2	3.20
e9	Linear	10%	2	3.33
e10	Linear	30%	2	3.42
e11	Linear	50%	2	3.72
e12	Linear	70%	2	4.12
e13	None	0%	3	3.09
e14	None	0%	4	3.12
e15	None	0%	5	3.14
e16	None	0%	6	3.16

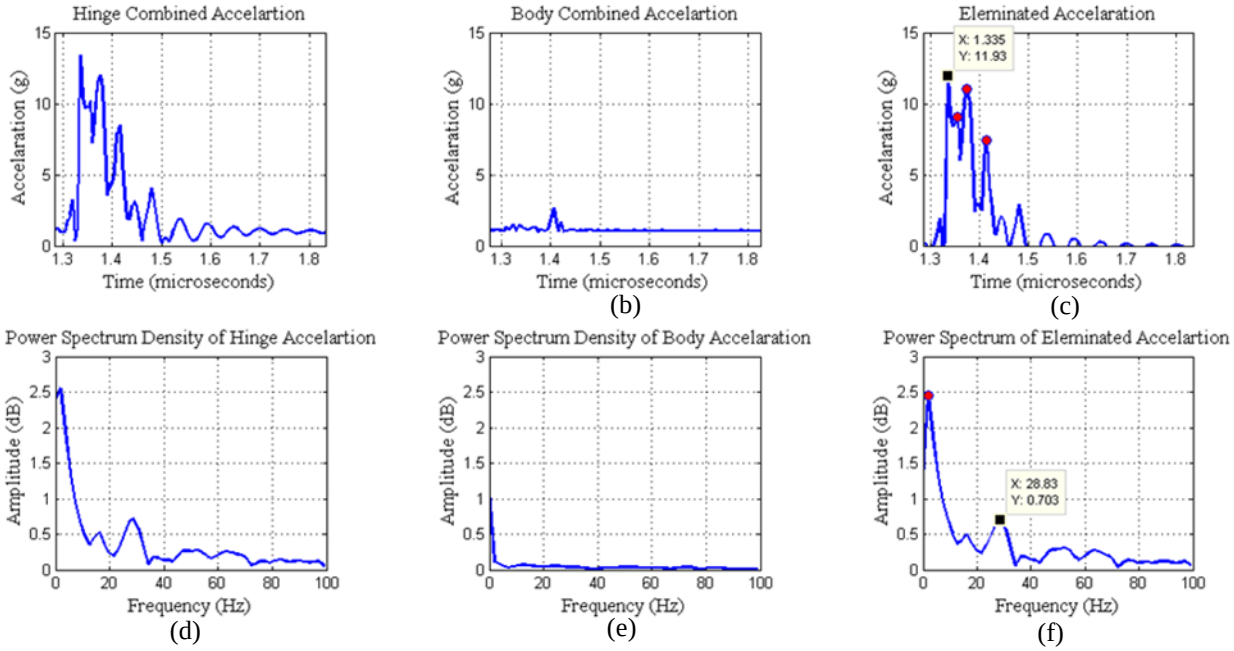

Figure 12. Results of Experiment 01

The mean values of the infill and shell experiments with 80 samples are presented in Table 2 and Table 3, respectively. Concerning the effect of infill density on combined accelerations in the time domain, directly proportional infill density and combined acceleration peak value for both of the honeycomb and linear infill patterns are found. Both of the patterns begin nearly at the same point but the effect of the honeycomb pattern is larger than the linear pattern in Figure 13. In the frequency domain, the honeycomb pattern's vibration frequency is higher than the linear patterns. They begin with the same 0% infill density. It is expected to be equal to 100%. Such behavior is seen on the graph in Figure 14.

The frequency difference is increasing in middle values for honeycomb and linear patterns. In short, as infill density increases, the vibration frequency increases.

In the frequency domain, peak magnitudes are exhibited a scattered image. No significant effect has been observed to indicate that any effect has occurred with increasing or decreasing of infill density. Peak magnitude is changeable in 0,6 and 1 dB which is shown in Figure 15. In time-domain peak values, as the number of shells increases, combined acceleration increases too. With 2 shells, it is nearly 12 g; it is greatly increased in 3 shells. After 3 shells, it is changeable between 18g and 19g which is shown in Figure 16. In the frequency domain, as the number of shells increases, peak frequency increases too, as it is seen in Figure 17. It has been seen in figures that it is possible to have the same peak frequency by increasing the number of shells. As shown in Figure 18, as the number of shells increases, peak magnitude increases too. But this value does not have a very big difference; it is changeable in 0.5dB and 1dB.

Table 2. Average Results of Infill Experiments

Ex.No	Infill		Time	Frequency	
	Pattern	Density	Value	Freq.	Mag.
e01	H	%0	11.497	27.387	0.719
e02	H	%5	15.401	37.477	0.890
e03	H	%10	17.588	41.802	0.735
e04	H	%30	19.147	70.631	0.645
e05	H	%50	19.902	73.153	0.800
e06	H	%70	20.267	75.946	0.848
e07	L	%0	11.692	26.306	0.682
e08	L	%5	15.367	33.153	0.835
e09	L	%10	17.215	38.198	0.961
e10	L	%30	19.045	51.171	0.749
e11	L	%50	18.396	69.550	0.777
e12	L	%70	19.274	75676	0.801

Table 3. Average Results of Shell Experiments

Ex.No	Infill Nof shells	Time Peak Value (g)	Frequency	
			Peak Freq. (Hz)	Peak Mag. (dB)
(e01+e02) /2	2	11.497	27.87	0.719
e13	3	17.845	36.396	0.864
e14	4	18.296	45.766	0.880
e15	5	18.489	46.657	0.907
e16	6	17.876	52.973	0.978

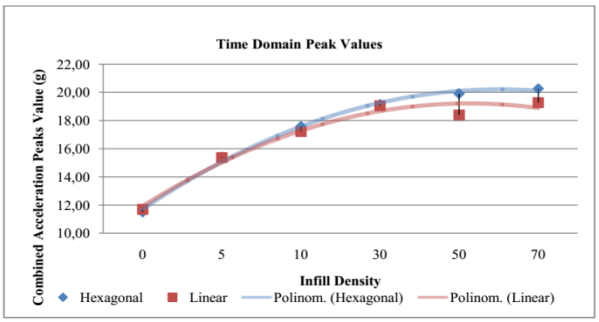

Figure 13. Effect of Infill Density in Acceleration Time Domain Peak Values

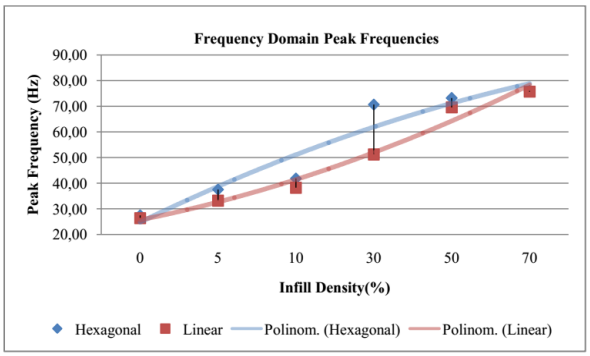

Figure 14. Effect of Infill Density on Peak Frequency

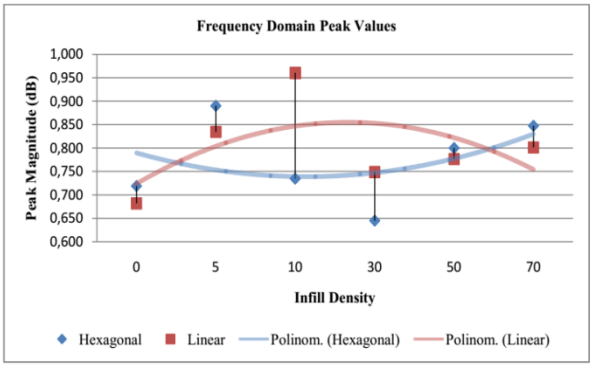

Figure 15. Effect of Infill Density on Peak Magnitude

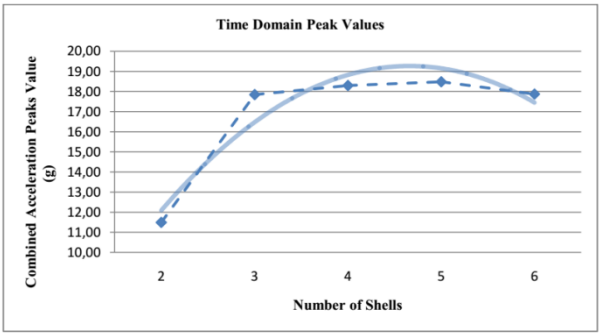

Figure 16. Effect of Number of Shells on Combined Acceleration

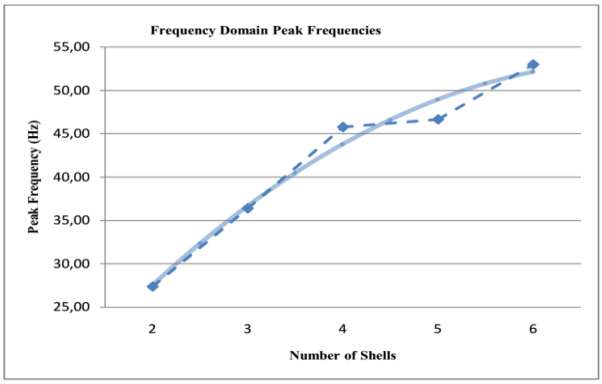

Figure 17. Effect of Shells on Peak Frequency

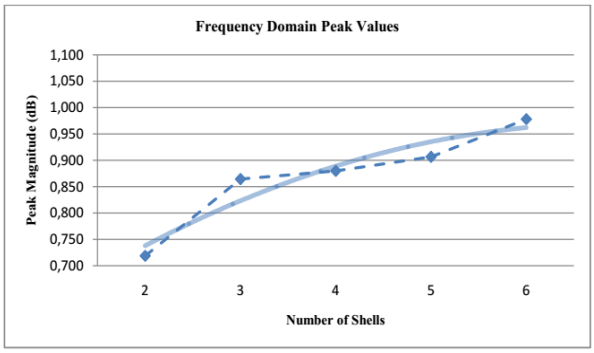

Figure 18. Effect of Number of Shells on Peak Magnitude

The findings obtained as a result of experiments with the system measuring the amount of energy consumption are presented in Figure 19. The infill density of the hinge used in the experiments is 30%. According to the findings, as the number of shells increases, the amount of energy consumption increases. The highest energy consumption in the graph belongs to a 6-shell honeycomb system and is worth 9,38Ws.

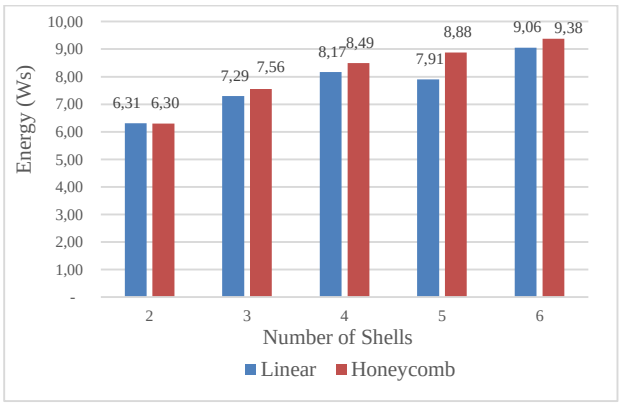

Figure 19. Effect of Number of Shells on Energy Consumption for Linear and Honeycomb Flexible Hinges

The results obtained by changing the infill density of the hinge used in the experiments are given in Figure 20. According to the findings, as the percentage of filling increases, the amount of energy consumption increases. Hinge with a 70% fill rate and is 11,25 Ws. (Watt second) It is seen that these values are compatible with oscillation values.

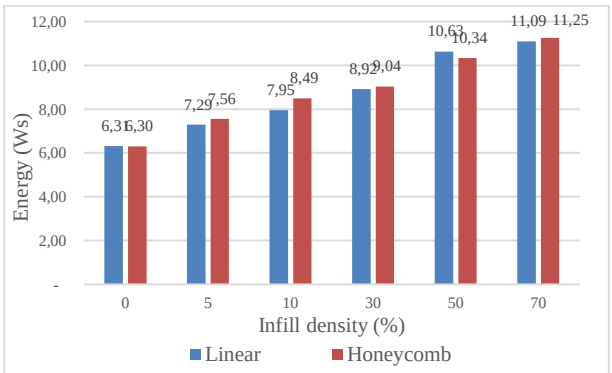

Figure 20. Effect of Infill Density on Energy Consumption for Linear and Honeycomb Flexible Hinges

4. CONCLUSION

In this paper, a single axis flexible hinge is produced by 3d printer and a hinge tester mechanism is designed to measure energy storage on hinges. Because of the advantages, hinge production with 3d printer is suggested as a serial production method. Forces and vibrations generated by hinges which have different printing characteristics are measured with the accelerometer. An increase in frequency means that it can discharge stored energy and recover fast. Hinges' infill pattern, infill density, and the number of shells are changed and the effects of these features on the frequency and combined acceleration are investigated.

About the effects of infill density on combined accelerations in the time domain; it has been found that infill density increases combined acceleration peak values in the time domain. This result is valid for both honeycomb and linear infill patterns. But the effect of the honeycomb pattern is larger than the linear pattern. In the frequency domain, the honeycomb pattern's vibration frequency is higher than the linear patterns. They begin at the same point in 0% infill density; it is expected to be equal in 100% infill density. Briefly, as infill density increases, the vibration frequency increases. In the frequency domain, peak magnitudes have exhibited a scattered image. No significant effect has been observed to indicate that any effect has occurred by increasing or decreasing infill density. Peak magnitude changes between 0, 6, and 1 dB. When numbers of shells effects are investigated, in the time domain as the number of shells increases, combined acceleration increases too. In the frequency domain, as the number of shells increases, peak frequency increases too. Also, it is possible to have the same peak frequency by increasing the number of shells instead of increasing infill density. And also, it has been concluded that the hinge, which has the highest energy storage capacity at the lowest cost, will have a honeycomb filling shape, 30% filler, and four shells. As a result of energy consumption levels with hinges, it has been observed that energy consumption increases as infill density and number of shell values increase. It is seen that these values are compatible with oscillation values.

This study will be a light for wearable machines that include hinge while estimating the mechanical behaviors and optimizing its mechanical parts. If a fast aggregation (which is an important feature for prostheses) is desired, a hinge that provides a high frequency can be preferred.

ACKNOWLEDGMENT

This study is performed under the project named Limb Design with Wearable Soft Robotic Actuator for Amputees", UBAP06 2015/TP005 Project at Uşak University. The 3D printer and other measurement instruments are supplied from the Electronics Laboratory of Uşak University Technical Sciences Vocational School.

DECLARATION OF ETHICAL STANDARDS

The authors of this article declare that the materials and methods used in this study do not require ethical committee permission and/or legal-special permission.

AUTHORS' CONTRIBUTIONS

Mine SEÇKİN: Perofrmed the experiments and analyse the results. Wrote the manuscript.

Necla YAMAN TURAN: Analysed the results.Wrote the manuscript

Ahmet Çağdaş SEÇKİN: Measurement circuit design and prepare signal processing program.

CONFLICT OF INTEREST

There is no conflict of interest in this study.

REFERENCES

[1] N. Lobontiu, ***Compliant mechanisms: design of flexure hinges***. CRC press, (2002).

[2] R. Mutlu, G. Alici, M. in het Panhuis, and G. Spinks, "Effect of flexure hinge type on a 3D printed fully compliant prosthetic finger," in 2015 IEEE International Conference on Advanced Intelligent Mechatronics (AIM), 790–795, (2015).

[3] R. Mutlu, G. Alici, M. in het Panhuis, and G. M. Spinks, "3D printed flexure hinges for soft monolithic prosthetic fingers," ***Soft Robotics***, 3(3):120–133, (2016).

[4] J. C. S. Terry, "Plastic hinge and method of making the same," , (1961).

[5] B. T. Cheok, K. Y. Foong, A. Y. C. Nee, and C. H. Teng, "Some aspects of a knowledge-based approach for automating progressive metal stamping die design," ***Computers in Industry***, 24(1):81–96, (1994).

[6] K. S. Pister, M. W. Judy, S. R. Burgett, and R. S. Fearing, "Microfabricated hinges," ***Sensors and Actuators*** A: Physical, 33(3): 249–256, (1992).

[7] H. Ding, S. J. Chen, and K. Cheng, "Two-dimensional vibration-assisted micro end milling: cutting force modelling and machining process dynamics," Proceedings of the Institution of Mechanical Engineers, Part B: ***Journal of Engineering Manufacture***, 224(12): 1775–1783, (2010).

[8] K. Suzuki, I. Shimoyama, and H. Miura, "Insect-model based microrobot with elastic hinges," ***Journal of Microelectromechanical Systems***, 3(1):4–9,(1994).

[9] K. Cai, Y. Tian, F. Wang, D. Zhang, and B. Shirinzadeh, "Development of a piezo-driven 3-DOF stage with T-shape flexible hinge mechanism," ***Robotics and Computer-Integrated Manufacturin***g, 37:125–138, (2016).

[10] B. Siciliano and O. Khatib, ***Springer Handbook of Robotics. Springer***, (2016).

[11] A. P. Neukermans and T. G. Slater, "Micromachined hinge having an integral torsion sensor," Jul. 15, (1997).

[12] L. Qiu, L. Liang, D. Li, and G. Xu, "Theoretical and experimental study on FBG accelerometer based on multi-flexible hinge mechanism," ***Optical Fiber Technology***, 38:142–146, (2017).

[13] M. Liu, W. Wang, H. Song, S. Zhou, and W. Zhou, "A high sensitivity FBG strain sensor based on flexible hinge," ***Sensors***, 19(8):1931, (2019).

[14] Y. Li, H. Li, T. Cheng, X. Lu, H. Zhao, and P. Chen, "Note: Lever-type bidirectional stick-slip piezoelectric actuator with flexible hinge," ***Review of Scientific Instruments***, 89(8): 086101, (2018).

[15] F. Qin et al., "Actively controlling the contact force of a stick-slip piezoelectric linear actuator by a composite flexible hinge," ***Sensors and Actuators A: Physical***, 299: 111606, (2019).

[16] F. Lotti and G. Vassura, "A novel approach to mechanical design of articulated fingers for robotic hands," in Intelligent Robots and Systems, 2002. IEEE/RSJ International Conference on, , 2: 1687–1692, (2002)

[17] B. Miloradović, B. Çürüklü, M. Vujović, S. Popić, and A. Rodić, "Low–cost anthropomorphic robot hand with elastic joints–early results," (2015).

[18] Y. Ogahara, Y. Kawato, K. Takemura, and T. Maeno, "A wire-driven miniature five fingered robot hand using elastic elements as joints," in Proceedings 2003 IEEE/RSJ International Conference on Intelligent Robots and Systems (IROS 2003), 3:2672–2677. (2003).

[19] L. Biagiotti, F. Lotti, C. Melchiorri, and G. Vassura, "Mechatronic design of innovative fingers for anthropomorphic robot hands," in 2003 IEEE International Conference on Robotics and Automation, 3: 3187–3192, (2003).

[20] Z. Zhu, X. Zhou, R. Wang, and Q. Liu, "A simple compliance modeling method for flexure hinges," ***Science China Technological Sciences***, 58(1):56–63, (2015).

[21] M. C. Carrozza et al., "The SPRING hand: development of a self-adaptive prosthesis for restoring natural grasping," ***Autonomous Robots,*** 16(2):125–141, (2004).

[22] M. Andrejašic, "Mems accelerometers," in *University of Ljubljana. Faculty for mathematics and physics, Department of physics, Seminar*, (2008).